Development 139, 4633-4643 (2012) doi:10.1242/dev.086991

Gbx2 regulates thalamocortical axon guidance by modifying the LIM and Robo codes

Mallika Chatterjee[1,*], Kairong Li[1,*], Li Chen[1,*], Xu Maisano[1], Qiuxia Guo[1], Lin Gan[2] and James Y. H. Li[1,‡]

SUMMARY

Combinatorial expression of transcription factors forms transcriptional codes to confer neuronal identities and connectivity. However, how these intrinsic factors orchestrate the spatiotemporal expression of guidance molecules to dictate the responsiveness of axons to guidance cues is less understood. Thalamocortical axons (TCAs) represent the major input to the neocortex and modulate cognitive functions, consciousness and alertness. TCAs travel a long distance and make multiple target choices en route to the cortex. The homeodomain transcription factor Gbx2 is essential for TCA development, as loss of *Gbx2* abolishes TCAs in mice. Using a novel TCA-specific reporter, we have discovered that thalamic axons are mostly misrouted to the ventral midbrain and dorsal midline of the diencephalon in *Gbx2*-deficient mice. Furthermore, conditionally deleting *Gbx2* at different embryonic stages has revealed a sustained role of Gbx2 in regulating TCA navigation and targeting. Using explant culture and mosaic analyses, we demonstrate that *Gbx2* controls the intrinsic responsiveness of TCAs to guidance cues. The guidance defects of *Gbx2*-deficient TCAs are associated with abnormal expression of guidance receptors Robo1 and Robo2. Finally, we demonstrate that Gbx2 controls Robo expression by regulating LIM-domain transcription factors through three different mechanisms: Gbx2 and Lhx2 compete for binding to the *Lmo3* promoter and exert opposing effects on its transcription; repressing *Lmo3* by Gbx2 is essential for Lhx2 activity to induce *Robo2*; and Gbx2 represses *Lhx9* transcription, which in turn induces *Robo1*. Our findings illustrate the transcriptional control of differential expression of Robo1 and Robo2, which may play an important role in establishing the topography of TCAs.

KEY WORDS: Thalamocortical projections, Transcription factor, LIM domain proteins, Robo, Axon guidance, Mouse

INTRODUCTION

The assembly of neural circuits in the central nervous system exhibits remarkable precision. Significant progress has been made in our understanding of the extrinsic signaling mechanisms that regulate axon pathfinding, as well as intrinsic determinants, such as transcription factors, that control the identity of neurons (O'Donnell et al., 2009). However, far less is understood about the transcriptional control of intrinsic responsiveness to guidance cues that lead to proper wiring of the brain.

The thalamus plays a pivotal role in integrating and processing visual, auditory, sensory and motor information to and from the cortex (Jones, 2007). During embryogenesis, thalamic axons, known as thalamocortical axons (TCAs), have to navigate along a complex path to reach the cerebral cortex. In mouse embryos, TCAs first grow rostrally through the prethalamus, reaching the border between the diencephalon and telencephalon, where they make a sharp turn to enter the ventral telencephalon at embryonic day (E) 12.5 (López-Bendito and Molnar, 2003; Garel and Rubenstein, 2004). By E14.5, TCAs reach the junction between the ventral and dorsal telencephalon, and then turn dorsally and extend to the intermediate zone and subplate below the cortical plate. The axons wait in the subplate before invading the overlying cortical plate and finally terminate in cortical layers IV and VI soon after birth (O'Leary and Koester, 1993). Each thalamic nucleus connects with a specific set of cortical areas, and subsequently TCAs from a given thalamic nucleus form a topographic map within a specific cortical area. It has been shown that TCAs are sorted in the ventral telencephalon, thus leading to the establishment of their topography (Métin and Godement, 1996; Molnar et al., 1998; Seibt et al., 2003; Powell et al., 2008). Genetic studies have demonstrated that Slit-Robo signaling plays an important role in the navigation of TCAs in the ventral telencephalon (Bagri et al., 2002; López-Bendito et al., 2007; Bielle et al., 2011a; Bielle et al., 2011b). Furthermore, it has been shown that Slit1 is involved in establishing the topography of TCAs in the ventral telencephalon (Bielle et al., 2011b). *Robo2* is broadly expressed in the developing thalamus, whereas the expression of *Robo1* is mainly restricted to the medial part of the thalamus (Bagri et al., 2002; López-Bendito et al., 2007). The differential expression of Robo1 and Robo2 in distinct groups of thalamic neurons may be important for the navigation and topographic sorting of TCAs.

Members of the LIM-homeodomain (LIM-HD) and basic helix-loop-helix (bHLH) transcription factor families are expressed in different domains of the thalamus, suggesting that these proteins may form combinatorial transcriptional codes to impart neuronal identity and connectivity to thalamic neurons (Nakagawa and O'Leary, 2001). It has recently been shown that LIM-HD factor Lhx2 directly binds to putative regulatory elements in the *Robo1* and *Robo2* loci, and negatively regulates their transcription (Marcos-Mondejar et al., 2012). However, how Lhx2 generates the different expression patterns of Robo1 and Robo2 in the thalamus by the same inhibitory regulation remains unclear. Expression of *Gbx2* (gastrulation brain homeobox gene 2) is initiated in postmitotic neurons of the mouse thalamus at E10.5 (Bulfone et al., 1993). Deletion of *Gbx2* causes severe defects in the histogenesis of the thalamus and an almost complete loss of TCAs (Miyashita-Lin et al., 1999; Hevner et al., 2002). We have recently shown that,

[1]Department of Genetics and Developmental Biology, University of Connecticut Health Center, 400 Farmington Avenue, Farmington, CT 06030-6403, USA. [2]Department of Ophthalmology, University of Rochester, School of Medicine and Dentistry, 601 Elmwood Avenue, Rochester, NY 14642, USA.

*These authors contributed equally to this work
‡Author for correspondence (jali@uchc.edu)

Accepted 25 September 2012

although all thalamic neurons express *Gbx2* during development, the onset and duration of *Gbx2* expression are highly variable among different thalamic nuclei (Chen et al., 2009). These observations underscore the importance of *Gbx2* in the regulatory network that coordinates thalamic neuron specification and connectivity.

In this study, we have examined *Gbx2* function in controlling TCA development. We demonstrate that *Gbx2* determines the initial directional outgrowth of TCAs into the prethalamus and their subsequent pathfinding to the cortex by regulating their responsiveness to guidance cues. We show that the guidance errors of *Gbx2*-deficient TCAs were associated with mis-regulation of Robo1 and Robo2 expression. We have identified *Lmo3* as a putative direct transcriptional target of Gbx2. Our genetic and molecular biological data collectively demonstrate that Gbx2 regulates the LIM transcriptional codes comprising Lhx2, Lhx9 and Lmo3, which subsequently control the differential expression of Robo1 and Robo2 in the thalamus.

MATERIALS AND METHODS

Mouse and tissue preparation

All animal procedures described herein were approved by the Animal Care Committee at the University of Connecticut Health Center. All mouse strains were maintained on an outbred genetic background. Noon of the day on which a vaginal plug was detected was designated as E0.5 in the staging of embryos. The knock-in $Gbx2^{creER}$ allele and $Gbx2^{floxed}$ conditional mutant allele ($Gbx2^{F}$) have been described previously (Li et al., 2002; Chen et al., 2009). To perform conditional deletion of *Gbx2*, 4-6 mg of tamoxifen (Sigma, St Louis, MO, USA) in corn oil was administered to pregnant females carrying $Gbx2^{creER/F}$; $R26R^{lacZ/+}$ by oral gavage. Two other mouse lines harboring the following mutant alleles were used in the study: $Lhx2^{-}$, a null allele of the *Lhx2* gene (Porter et al., 1997), and $Lmo3^{lacZ}$, which is a *lacZ* knock-in and also a null allele of the *Lmo3* gene (Tse et al., 2004).

Embryonic mouse brains were dissected in cold phosphate-buffered saline (PBS) and fixed in 4% paraformaldehyde (PFA) for 40 minutes. Brains were cryoprotected, frozen in OCT freezing medium (Sakura Finetek) and sectioned.

Histochemistry, immunofluorescence and in situ hybridization

Standard protocols were used for X-gal histochemistry, immunofluorescence and in situ hybridization, as described previously (Chen et al., 2010). Detailed protocols are available on the Li Laboratory website (http://lilab.uchc.edu/protocols/index.html). Primary antibodies used in the study were as follows: rabbit anti-GFP (Invitrogen), rat anti-GFP (Nacalai Tesque), rabbit anti-Lhx9 (Santa Cruz), mouse anti-Nefm (2H3-DSHB), and rabbit anti-Robo1 and rabbit anti-Robo2 (kind gifts from Dr Atsushi Tamada, Niigata University, Japan). Alexa fluorescent secondary antibodies (Invitrogen) were used.

Chimera analyses

Chimeric embryos were generated by aggregation of morula, which resulted from intercrosses between $Gbx2^{+/-}$ and $Gbx2^{creER/+}$ mice, and embryonic stem (ES) cells as described previously (Nagy et al., 2003). Chimeric embryos containing $Gbx2^{creER/+}$ or $Gbx2^{creER/-}$ cells were identified by the presence of EGFP fluorescence, and these two groups of embryos were further distinguished by PCR genotyping the $Gbx2^{-}$ and $Gbx2^{creER}$ alleles (Wassarman et al., 1997; Li et al., 2002).

Electrophoretic mobility shift assay (EMSA) and luciferase assay

EMSA was performed according to standard protocols (Buratowski and Chodosh, 2001; Kain and Ganguly, 2001). The functional EGFP:Gbx2 fusion protein was generated by fusing EGFP to the N terminus of Gbx2. The DNA probe sequence is: Lmo3-ab, 5′-GATAATTAAACTAATTAGTTCCCCTGTG; Lmo3-cd, 5′-TGCTTTGTACCTAATTAGTGTCCTTGGA (Gbx2-binding sequence is underlined). The oligo with scrambled binding sequence is: Lmo3-ef, GATAATTAAAATTCATAGTTCCCCTGTG; Lmo3-gh, TGCTTTGTACTAACATTGTGTCCTTGGA (scrambled binding sequence is underlined).

Luciferase reporter assay was performed in P19 embryonal carcinoma cells using a Dual-Luciferase Assay System (Promega). A 1.2 kb genomic DNA fragment containing two putative Gbx2-binding sites upstream of *Lmo3* transcription start site was cloned into a luciferase reporter *pGL3* (Promega). Full-length cDNAs for *Gbx2*, *EGFP:Gbx2*, *Lhx2*, *Lhx5*, *Lhx9*, *Otx2*, *Irx1* and *Lmo3* were cloned in a *CMV*-expression construct. Lipofectamine 2000 (Invitrogen) was used for transfection of P19 cells.

Explant co-culture and axonal tracing

Explant co-culture was performed as described previously (Bonnin et al., 2007). Explants were prepared from E13.5 $Gbx2^{creER/+}$; $R26R^{RFP/+}$ or $Gbx2^{creER/-}$; $R26R^{RFP/+}$ embryos that were given tamoxifen at E10.5 so that the thalamic neurons and their processes were labeled with RFP. Brain explants were co-cultured with aggregates of 293T cells transfected with *CMV-EGFP* alone or *CMV-EGFP* and *CMV-SLIT2* in Matrigel (BD Biosciences). After 48 hours, the cultures were mounted on slides and imaged. Axon outgrowth originating from proximal and distal quadrants was determined by measuring the total RFP fluorescence associated with the axon-occupied area using ImageJ software (NIH) as described previously (Brose et al., 1999). Statistical difference between proximal and distal areas was determined by chi-square test.

RESULTS

Gbx2 determines the initial trajectory of TCAs

We have previously generated a $Gbx2^{creER}$ allele, which contains a *creER-ires-EGFP* sequence inserted into the 5′-untranslated region of the *Gbx2* locus so that the expression of both creER and EGFP mimics the endogenous *Gbx2* expression (Chen et al., 2009). In embryos carrying the $Gbx2^{creER}$ allele, TCAs were specifically labeled by EGFP, providing an excellent tool with which to study TCA development. Immunohistochemistry for GFP showed that TCAs extended rostrally through the prethalamus reaching the diencephalic-telencephalic border in $Gbx2^{creER/+}$ embryos at E12.5 (Fig. 1A). Strikingly, the majority of GFP^{+} neurons projected dorsally and caudally, and few GFP^{+} axons were found in the prethalamus in E12.5 $Gbx2^{creER/-}$ embryos, which are deficient for Gbx2 (Fig. 1B). In $Gbx2^{creER/+}$ embryos at E14.5, immunofluorescence for GFP and neurofilament (NF) showed that TCAs were specifically labeled by GFP and GFP immunoreactivity was absent from the fasciculus retroflexus (FR) tract, which originates from the habenula (Fig. 1C). However, in $Gbx2^{creER/-}$ embryos, GFP^{+} thalamic axons were mostly misrouted and abnormally present in the FR tract (Fig. 1D). To rule out the possibility that the misrouted GFP^{+} axons resulted from ectopic expression of GFP in $Gbx2^{creER/-}$ embryos, we performed retrograde labeling by inserting DiI and DiA crystals in the ventral midbrain and dorsal midline of the diencephalon, respectively. In control embryos, few thalamic neurons were labeled by either DiI or DiA (supplementary material Fig. S1A-B″,E). By contrast, in $Gbx2^{creER/-}$ embryos, DiI and DiA backfilled neurons were abundantly found inside the thalamus, in additional to their normal presence in the habenula, pretectum and prethalamus (supplementary material Fig. S1C-D″,F). In agreement with the previous findings (Miyashita-Lin et al., 1999; Hevner et al., 2002), TCAs were mostly absent in the cortex of $Gbx2^{creER/-}$ embryos at E16.5 (Fig. 1F). Therefore, our data demonstrate that *Gbx2* is essential for determining the initial trajectory of TCAs. In the absence of *Gbx2*, most thalamic axons abnormally project to the ventral midbrain along the FR tract or dorsal midline of the diencephalon, resulting in the loss of TCAs.

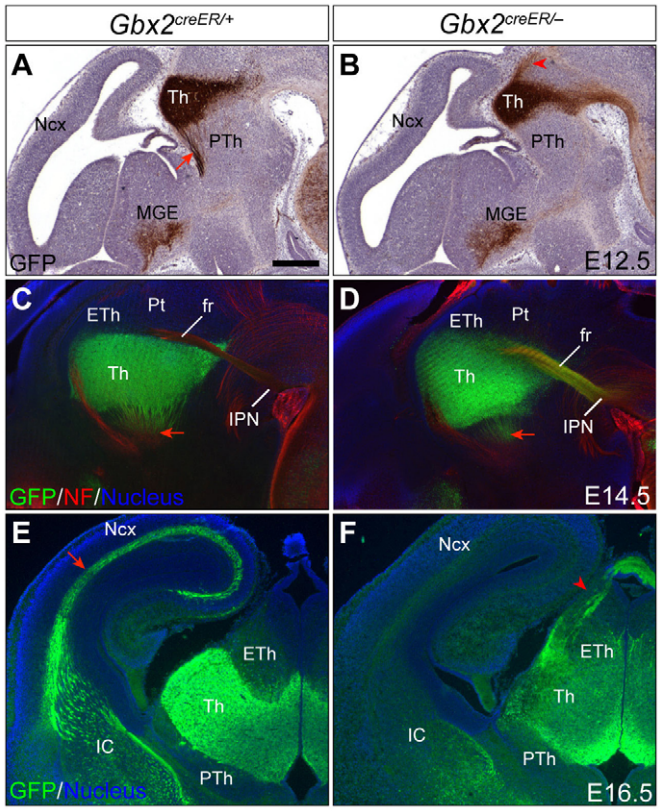

Fig. 1. Thalamic neurons abnormally project caudally and dorsally in *Gbx2*-deficient embryos. (**A**,**B**) GFP immunohistochemistry on sagittal sections of $Gbx2^{creER/+}$ (A) and $Gbx2^{creER/–}$ (B) embryos at E12.5. *Gbx2* is also expressed in the medial ganglionic eminence (MGE). (**C**,**D**) Double immunofluorescence for GFP and neurofilament (NF) on sagittal sections of $Gbx2^{creER/+}$ (C) and $Gbx2^{creER/–}$ (D) embryos at E14.5. (**E**,**F**) Immunofluorescence for GFP on coronal sections of $Gbx2^{creER/+}$ (E) and $Gbx2^{creER/–}$ (F) embryos at E16.5. Arrows indicate normal TCAs; arrowheads show aberrant projections. ETh, epithalamus; fr, fasciculus retroflexus; IPN, interpeduncular nucleus; Ncx, neocortex; Pt, pretectum; PTh, prethalamus; Th, thalamus. Scale bar: 400 μm in A,B; 423 μm in C,D; 332 μm in E,F.

Gbx2 continues to regulate the navigation of TCAs after they pass the prethalamus

Gbx2 expression persists in many thalamic neurons (Jones and Rubenstein, 2004; Chen et al., 2009). To investigate whether prolonged *Gbx2* expression is required for TCAs to properly navigate to the cortex, we deleted *Gbx2* by administering tamoxifen to $Gbx2^{creER/F}$ embryos at E13.5, when most TCAs have passed the prethalamus. The conditional knockout (CKO) embryos are designated as *Gbx2*-CKO. Interestingly, removing *Gbx2* at E9.5 or E13.5 resulted in abnormal trajectories of TCAs within the diencephalons, as found in $Gbx2^{creER/–}$ embryos (Fig. 2B; Fig. 3D), indicating that *Gbx2* controls the axonal trajectory of newly generated thalamic neurons at various stages. Additional guidance defects of TCAs were detected in E15.5 *Gbx2*-CKO embryos that were given tamoxifen at E13.5. In these mutants, many GFP^+ TCA fibers failed to enter the ventral telencephalon and instead projected towards the ventral midline of the hypothalamus (Fig. 2D,J). Furthermore, some GFP^+ fibers abnormally crossed over the TCA bundle at the entry of the internal capsule (Fig. 2F,J). As described previously (Lund and Mustari, 1977; Rakic, 1977), TCAs mostly remain in the subplate before invading the overlying cortical plate in control embryos at E15.5 (Fig. 2G). However, increased number of TCAs were found in the cortical plate in *Gbx2*-CKO mutants at E15.5 (Fig. 2H,J). Taken together, these results demonstrate that, in addition to its crucial role in regulating the initial trajectory of TCAs, *Gbx2* continues to regulate the navigation of TCAs and the timing to innervate the cortical plate.

Gbx2 controls the intrinsic responsiveness of thalamic axons to guidance cues

We have previously demonstrated that *Gbx2* has a non-cell-autonomous function in development of the thalamus (Chen et al., 2009). We thus investigated the cell autonomy of *Gbx2* function in TCA development. Because of the mosaic nature of creER-mediated recombination induced by tamoxifen, the thalamus in $Gbx2^{creER/F}$; $R26R^{lacZ/+}$ embryos that were given tamoxifen consisted of a mixture of $Gbx2^{creER/F}$ (functionally wild type) and $Gbx2^{creER/–}$ (*Gbx2*-deficient) cells as described previously (Chen et al., 2009) (supplementary material Fig. S2). Using a RFP cre-reporter line (Madisen et al., 2010), we showed that RFP+ axons, which were derived from recombined neurons (presumably *Gbx2* deficient), abnormally projected to dopaminergic neurons in the ventral midbrain via the FR tract (Fig. 3A,B). Furthermore, thalamic efferents with abnormal trajectories appeared to originate from recombined cells, whereas non-recombined cells gave rise to normal TCAs in E13.5 $Gbx2^{creER/F}$; $R26R^{lacZ/+}$ embryos that received tamoxifen at E9.5 (Fig. 3D). These observations suggest a cell-autonomous requirement for *Gbx2* in controlling the trajectory of thalamic axons. Because of the lack of anti-Gbx2 antibodies, we could not directly identify the individual *Gbx2*-deficient thalamic neurons in the mosaic embryos. To follow the behavior of *Gbx2*-deficient neurons, we generated chimeric embryos by aggregating $Gbx2^{creER/–}$ embryos with wild-type ES cells. In control chimeric embryos that were composed of wild-type and $Gbx2^{creER/+}$ cells, $Gbx2^{creER/+}$ neurons (GFP^+) projected rostrally into the prethalamus at E11.5 (Fig. 3E-G). A few processes that did extend into the epithalamus traveled only for a short distance and became tangled (Fig. 3F), suggesting that TCAs are inhibited from entering the epithalamus. In mutant chimeric embryos, $Gbx2^{creER/–}$ (GFP^+) cells intermingled with wild-type ($GFP^–$) cells in the MZ (Fig. 3H-J), demonstrating that loss of *Gbx2* does not alter cell adhesion properties. Significantly, $Gbx2^{creER/–}$ thalamic axons extended dorsally into the epithalamus and pretectum, and mostly failed to grow into the prethalamus (Fig. 3H-J). Altogether, our results demonstrate that *Gbx2* acts cell-autonomously to control the initial trajectory of TCAs.

The guidance errors of TCAs found in mosaic mutants suggest that loss of *Gbx2* alters the intrinsic responsiveness of TCAs to guidance cues. *Slit1* and *Slit2*, which encode secreted guidance proteins, are known to regulate TCA entry and navigation into the ventral telencephalon (Bagri et al., 2002). Explant assays have shown that Slit2 inhibits the outgrowth of thalamic axons and acts as a repellant to thalamic axons (Bonnin et al., 2007; López-Bendito et al., 2007; Braisted et al., 2009). To investigate whether loss of *Gbx2* alters the responsiveness of TCAs to Slit2, we performed explant co-culture experiments. As expected, control ($Gbx2^{creER/+}$) thalamic axons displayed avoidance to Slit2-expressing cells (Fig. 3K,M). However, $Gbx2^{creER/–}$ thalamic neurons mostly failed to respond to Slit2 (Fig. 3L,M). Altogether, our results demonstrate that *Gbx2* regulates the intrinsic responsiveness of TCAs to guidance cues.

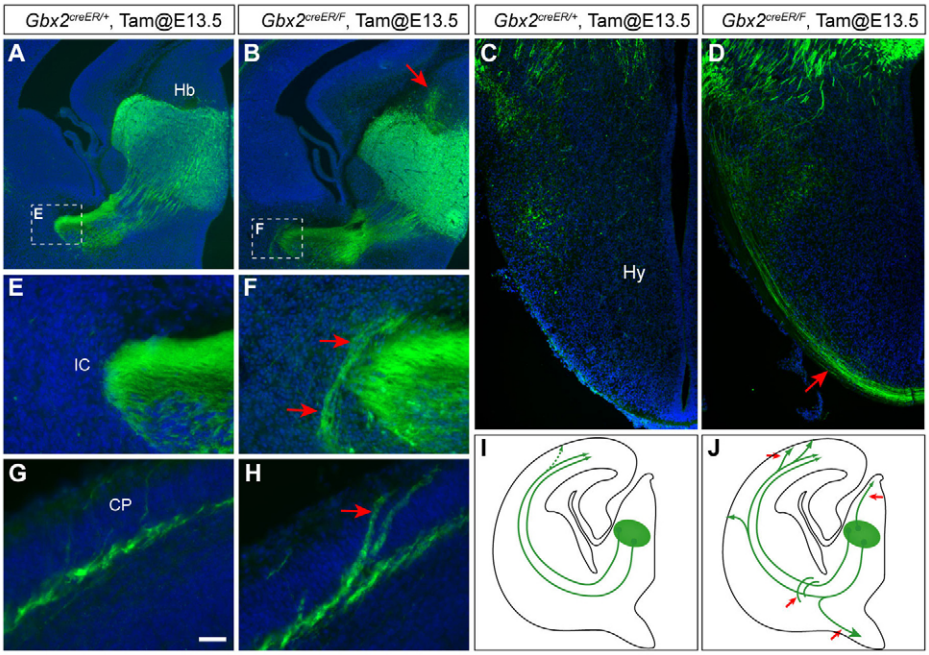

Fig. 2. Deleting *Gbx2* at E13.5 results in TCA pathfinding defects. (**A-H**) Immunofluorescence for GFP on coronal sections of E15.5 $Gbx2^{creER/F}$ embryos that received tamoxifen at E13.5. Boxed areas are magnified as indicated. Arrows indicate abnormal TCAs in the habenula (Hb) (B), in the hypothalamus (Hy) (D), at the entry of internal capsule (IC) (F) and within the cortical plate (CP) (H). (**I**,**J**) Schematic summary of the pathfinding defects of TCAs in different brain regions of *Gbx2*-CKO mutants. Scale bar: 250 μm in A,B; 50 μm in C-F; 100 μm in G,H.

Gbx2 regulates the expression of Robo1 and Robo2 in thalamic neurons

The guidance defects at the junction between the diencephalon and the telencephalon in *Gbx2*-CKO mutants share similarities to those described in mutants lacking Slit or Robo genes (Bagri et al., 2002; López-Bendito et al., 2007). Furthermore, the failure to respond to Slit2 suggests that loss of *Gbx2* may alter Robo expression in the thalamus. As described previously (Bagri et al., 2002; López-Bendito et al., 2007), although both *Robo1* and *Robo2* are expressed in the medial region of the thalamus, only *Robo2* transcripts are present in the lateral wall of the thalamus (Fig. 4A-B′). In the absence of *Gbx2*, *Robo1* transcripts and proteins were abnormally detected in the lateral area of the thalamus, as well as in the misrouted thalamic axons in the epithalamus (Fig. 4C,C′). *Robo2* transcripts and proteins were greatly reduced in the thalamus without *Gbx2* (Fig. 4D,D′). In control embryos at E15.5, most of the GFP^+ TCAs displayed only low levels of Robo1 (Fig. 4E). By contrast, the expression of Robo1 proteins was noticeably enhanced in TCAs within the cortex of *Gbx2-CKO* embryos (Fig. 4F). Significantly, enhanced Robo1 expression was also detected in the TCAs that precociously invaded the cortical plate in *Gbx2*-CKO embryos (Fig. 4F), demonstrating a cell-autonomous requirement for *Gbx2* in repressing Robo1 expression. Therefore, *Gbx2* is essential for establishing the distinct expression patterns of Robo1 and Robo2 in the developing thalamus.

Lmo3 is a direct transcriptional target of Gbx2

As it has been shown that *Robo1* and *Robo2* are direct transcriptional targets of Lhx2 (Marcos-Mondejar et al., 2012), we studied the interaction between Lhx2 and Gbx2 in regulating *Robo1* and *Robo2*. We found that the expression of *Lhx2* was unaltered in the thalamus lacking *Gbx2* at E12.5 (data not shown), demonstrating that Gbx2 does not regulate Lhx2 at the mRNA level. The function of LIM-HD transcription factors can be negatively regulated by LIM-domain-only (LMO) proteins, which compete for LIM-HD obligate co-factor, LIM domain-binding protein (Ldb) (Bach, 2000). Significantly, loss of *Gbx2* led to upregulation of *Lmo3*, one of the four members of mammalian LMO genes (Tse et al., 2004). *Lmo3* is normally expressed in the epithalamus and pretectum, and was ectopically expressed in the thalamus of $Gbx2^{creER/-}$ embryos at E12.5 (Fig. 5A,B). In E12.5 $Gbx2^{creER/F}$; $R26R^{lacZ/+}$ embryos that received tamoxifen at E10.5, ectopic *Lmo3*-expressing cells displayed a ‘salt-and-pepper’ pattern of expression in the thalamus (Fig. 5C). This pattern of ectopic expression is consistent with a cell-autonomous function of *Gbx2* in repressing *Lmo3* in mosaic mutant thalamus.

To investigate whether Gbx2 may directly regulate *Lmo3* transcription, we searched for putative Gbx2 binding sequences in the evolutionarily conserved genomic DNA sequence upstream of the *Lmo3* promoter using rVISTA (Loots et al., 2002; Berger et al., 2008). Two Gbx2-binding sites were identified within a highly conserved 510 bp DNA sequence located 1.2 kb upstream of the *Lmo3* transcription start site (Fig. 5E). Electrophoretic mobility shift assay (EMSA) showed that Gbx2 specifically bound to these two putative binding sites (Fig. 5F; data not shown). Therefore, Gbx2 is required to inhibit *Lmo3* transcription in the thalamus probably by binding to the *Lmo3* promoter.

Lmo3 is a feedback inhibitor of Lhx2

Interestingly, Gbx2 and Lhx2 proteins have almost identical DNA-binding sequences (Berger et al., 2008), and similar temporospatial expression patterns in the thalamus (Nakagawa and O’Leary, 2001; Lakhina et al., 2007). These observations raise the interesting possibility that Gbx2 and Lhx2 might have opposing functions in regulating the transcription of *Lmo3* by competing for binding to the same sequence in the *Lmo3* promoter. Using a luciferase reporter assay in P19 cells, we showed that Lhx2 robustly activated the *Lmo3* promoter, while Gbx2 efficiently inhibited the activity of Lhx2 (Fig. 5G,H). The transactivation was specific to Lhx2 and Lhx5, whereas other homeodomain transcription factors that were tested had no activity in the same assay (Fig. 5G). Moreover, mutating any of the two putative Gbx2/Lhx2-binding sites completely abolished the activation by Lhx2 (Fig. 5G). This is in agreement with the report that LIM-HD transcriptional complexes

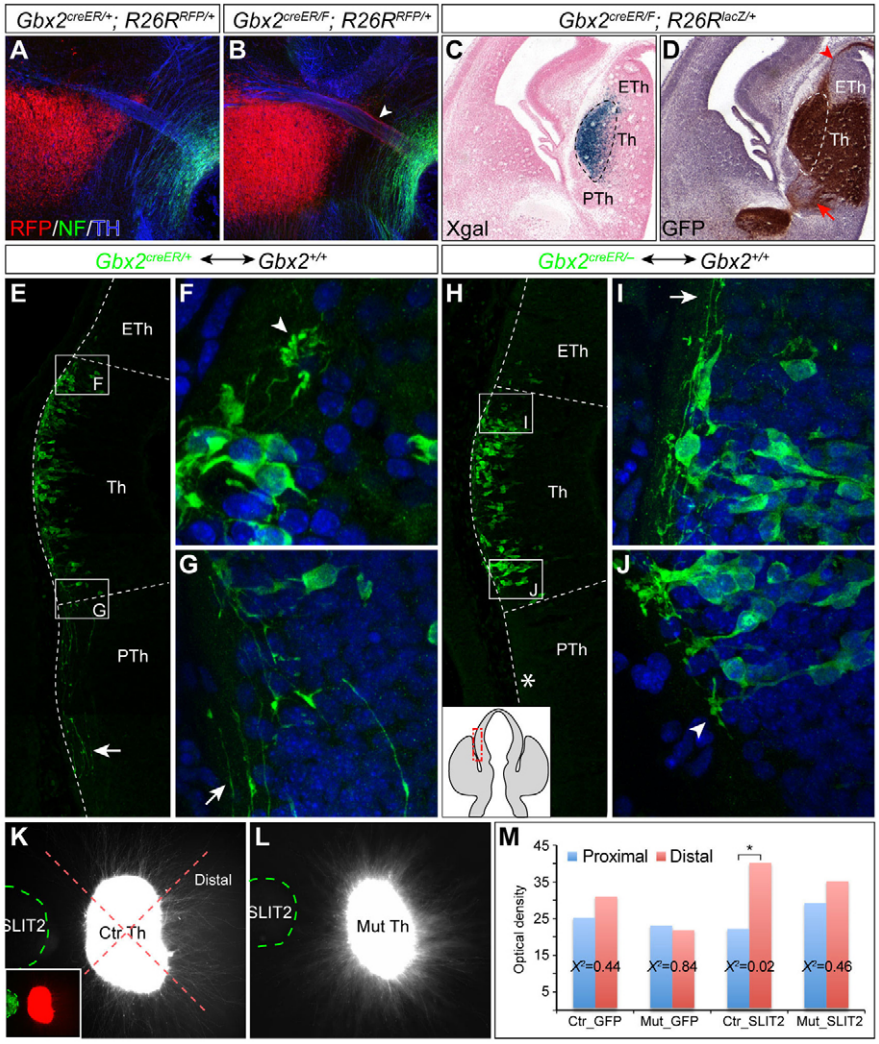

Fig. 3. *Gbx2* regulates the intrinsic responsiveness of thalamic axons to guidance cues during TCA development. (**A**,**B**) Immunofluorescence for RFP, neurofilament (NF) and tyrosine hydroxylase (TH) on sagittal sections of E14.5 embryos that received tamoxifen at E10.5. The arrowhead indicates abnormal RFP$^+$ thalamic axons in the fasciculus retroflexus tract. (**C**,**D**) X-gal staining (C) and GFP immunohistochemistry (D) on adjacent coronal brain sections of E14.5 *Gbx2*$^{creER/F}$; *R26R*$^{lacZ/+}$ embryos that were given tamoxifen at E9.5. Axons of aberrant trajectories (arrowhead) are mainly derived from recombined cells (broken line), whereas normal TCAs (arrow) are derived from non-combined cells. (**E-J**) Immunofluorescence for GFP on coronal sections of E11.5 chimeric embryos. The boxed areas are magnified in F,G,I,J as indicated. Arrows indicate rostral extension of thalamic axons; arrowheads mark abnormal tangling of axons. The red box in the inset in H indicates the areas shown in E and H. (**K**,**L**) Thalamic explants from *Gbx2*$^{creER/+}$; *R26R*^{RFP} (K) and *Gbx2*$^{creER/–}$; *R26R*^{RFP} (L) embryos that received tamoxifen at E10.5 were co-cultured with SLIT2-expressing cells (outlined by a green dashed line). Cell bodies and their processes are labeled by RFP. Broken red lines show the division of the proximal and distal quadrants; the inset shows a color image of K where Slit2$^+$ cells and the explant are labeled by GFP and RFP, respectively. (**M**) Optical density (OD) of proximal and distal quadrants. The asterisk indicates significant difference.

bind to DNA with two 'half-binding sites' (Thaler et al., 2002; Lee et al., 2008). Finally, we showed that, in the presence of Lmo3 protein, Lhx2 failed to activate the transcription of the *Lmo3* promoter, demonstrating that Lmo3 can inhibit the transcriptional activity of Lhx2 (Fig. 5G).

To determine whether *Lhx2* is indeed responsible for inducing *Lmo3* in the *Gbx2*-deficient thalamus, we generated *Gbx2*$^{creER/creER}$; *Lhx2*$^{–/–}$ double mutants. In support of our model, ectopic expression of *Lmo3* in the thalamus was greatly reduced in *Gbx2*$^{creER/creER}$; *Lhx2*$^{–/–}$ embryos at E12.5 (Fig. 5D). Furthermore, in both *Lhx2*$^{–/–}$ and *Gbx2*$^{creER/creER}$; *Lhx2*$^{–/–}$ embryos, *Lmo3* expression was mostly lost in the ventral telencephalon (Fig. 5D; data not shown), demonstrating a requirement of *Lhx2* to induce *Lmo3* in this region. Therefore, our results show that Gbx2 and Lhx2 have opposite (negative and positive, respectively) functions in regulating *Lmo3* transcription, and Lmo3 acts as a feedback inhibitor of Lhx2 in the developing thalamus (Fig. 5I).

Ectopic expression of Lmo3 contributes to the loss of Robo2 in Gbx2-deficient thalamus

Based on the above model (Fig. 5I), we made the following two predictions: (1) inactivation of *Gbx2* would lead to functional disruption of Lhx2 through ectopic expression of *Lmo3*; (2) removal of *Lmo3* would restore defects caused by the disrupted Lhx2 function in *Gbx2* mutants. To test the first prediction, we examined whether loss of *Gbx2* or *Lhx2* leads to similar changes in *Robo1/2* expression. The previous study has only examined *Robo1/2* expression in the *Lhx2*-deficient thalamus at E14.5 (Marcos-Mondejar et al., 2012). Therefore, we compared the initial expression of *Robo1/2* in *Gbx2* and *Lhx2* mutant thalamus at E12.5. Similar to that found at later stages, ectopic expression of *Robo1* was found in the lateral-most region of the thalamus lacking either *Gbx2* or *Lhx2* (Fig. 6A-C). Interestingly, the level of *Robo2* expression was reduced in the thalamus in *Lhx2*$^{–/–}$ embryos, similar to that found in *Gbx2*$^{creER/–}$ embryos, at E12.5 (Fig. 6D-F). These findings are consistent with our model that Gbx2 is essential for Lhx2 function in the regulation of *Robo1* and *Robo2* expression in the thalamus.

We next examined whether removal of *Lmo3* could restore Lhx2 function as well as the expression of *Robo1/2* in *Gbx2* mutants. We used an *Lmo3*-null allele, *Lmo3*^{lacZ} (Tse et al., 2004), to generate *Gbx2* and *Lmo3* double mutants. In agreement with our prediction, the expression of *Robo2* was mostly restored in the thalamus of *Gbx2*$^{creER/creER}$; *Lmo3*$^{lacZ/lacZ}$ embryos at E13.5 (Fig. 6I,J). Unexpectedly, both *Gbx2*$^{creER/–}$ and *Gbx2*$^{creER/creER}$; *Lmo3*$^{lacZ/lacZ}$ embryos displayed similar ectopic expression of *Robo1* in the lateral wall of the thalamus at E13.5 (Fig. 6G,H). Our results demonstrate that the ectopic expression of *Lmo3* in *Gbx2* mutants

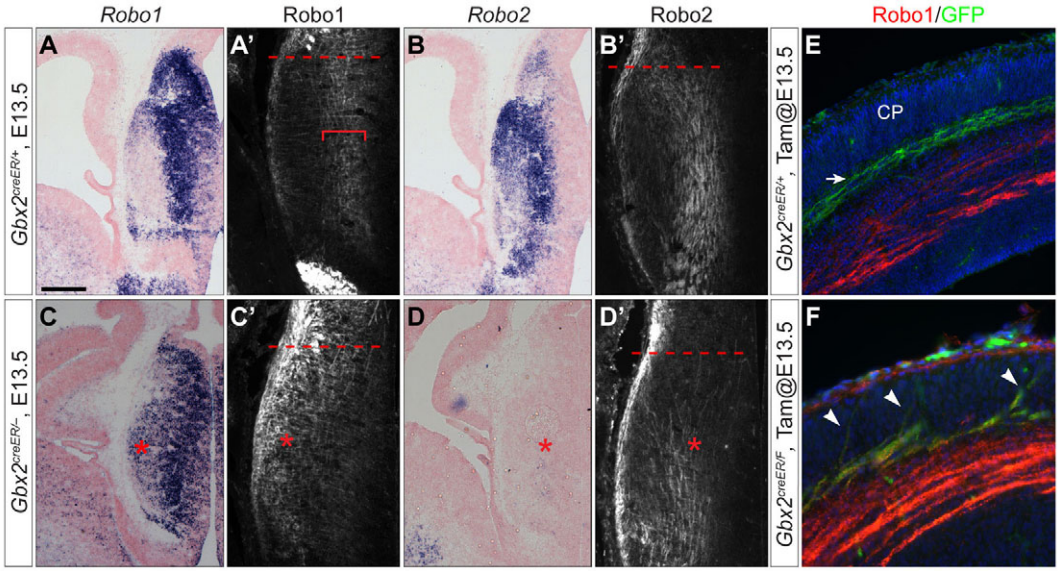

Fig. 4. *Gbx2* regulates the differential expression of *Robo1/2* in the developing thalamus. (**A-D**) In situ hybridization for Robo1 and Robo2 on coronal sections of E13.5 embryos. (**A′-D′**) Immunofluorescence for Robo1 and Robo2 on coronal sections of E13.5 brains. (**E**,**F**) Immunofluorescence for GFP and Robo1 on coronal sections of E15.5 brains of indicated genotypes. Brackets indicate Robo1 and Robo2 expression in the medial region of the thalamus; broken lines mark the dorsal-caudal border of the thalamus; asterisks show the ectopic expression of Robo1 and the loss of Robo2 in *Gbx2*-deficient thalamus; the arrow indicates the absence of Robo1 in TCAs beneath the cortical plate; arrowheads mark TCAs in the cortical plate (CP) of *Gbx2*-CKO mutants. Scale bar: 250 μm in A-D; 166 μm in A′-D′; 53 μm in E,F.

contributes to the loss of *Robo2*, but not to the ectopic expression of *Robo1*.

Gbx2 negatively regulates the transcription of Lhx9 in the thalamus

The failure to restore *Robo1* expression in $Gbx2^{creER/creER}$; $Lmo3^{lacZ/lacZ}$ embryos suggests that other factors in addition to Lmo3 and Lhx2 are involved in mediating Gbx2 function to regulate Robo1 in the thalamus. It has been reported that forced expression of *Lhx2* leads to downregulated expression of *Lhx9*, as well as *Robo1*, in the thalamus (Marcos-Mondejar et al., 2012). This prompted us to investigate whether Lhx9 may act downstream of Gbx2 or Lhx2 in regulating *Robo1* expression. We therefore first examined whether expression of *Lhx9* is altered due to loss of either *Lhx2* or *Gbx2*. As described previously (Nakagawa and O'Leary, 2001), *Lhx9* is broadly expressed but its transcripts are clearly absent in the lateral-most area of the thalamus at E12.5 (Fig. 7A). Without *Lhx2* or *Gbx2*, the expression domain of *Lhx9* was expanded to the lateral wall of the thalamus at E12.5 (Fig. 7B,C). Immunohistochemistry revealed the same abnormal expression of Lhx9 in the thalamus lacking *Lhx2* or *Gbx2* (data not shown). Therefore, both Lhx2 and Gbx2 are required to inhibit *Lhx9* expression in the lateral-most region of the thalamus.

To investigate the potential regulation of *Robo1* by Lhx9 in the developing thalamus, we performed in situ hybridization to compare the expression of *Robo1* and *Lhx9* on adjacent sections of control embryos at E13.5. Compared with the expression domain of *Robo1*, *Lhx9* transcripts were detected in cells closer to the ventricular surface (Fig. 7E-J), suggesting that *Lhx9* is induced before the onset of *Robo1* transcription. *Robo1* and *Lhx9* transcripts were mostly absent from the lateral-most area. Importantly, although the negative expression domains changed in size at different rostral-caudal levels of the thalamus, these two genes displayed an almost identical negative domain at any given position (Fig. 7E-J). In the absence of *Gbx2*, the expression domains of *Robo1* and *Lhx9* were similarly expanded to the lateral-most area of the thalamus (Fig. 7E′-J′). Finally, we found that removing *Lmo3* had no effect on the ectopic expression of *Robo1* and *Lhx9* in *Gbx2*-deficient thalamus (Fig. 7E″-J″). Therefore, Lhx2 and Gbx2 both negatively regulate Lhx9. Our expression analyses suggest that *Lhx9* may be responsible for the induction of *Robo1*, and the deregulation of *Lhx9* may contribute to the ectopic expression of *Robo1* in the thalamus lacking *Gbx2*.

DISCUSSION

In this study, by taking advantage of the EGFP expression that specifically labels TCAs in mice carrying the $Gbx2^{creER}$ allele, we have uncovered a hitherto unknown TCA phenotype of *Gbx2* mutants. We demonstrate that Gbx2 regulates the intrinsic responsiveness of TCAs, as least in part, by regulating the expression of Robo1 and Robo2 receptors. We identified an opposing activity between Gbx2 and Lhx2 in their direct control of *Lmo3* transcription. We showed that Lmo3 acts as a feedback inhibitor of Lhx2. Using genetic and molecular biological studies, we have identified the mechanisms by which Gbx2 regulates the LIM code in controlling *Robo1* and *Robo2* expression in thalamic neurons.

Regulation of the initial trajectory of TCAs

Although it is known that *Gbx2* is essential for the formation of TCAs, the mechanism underlying the Gbx2 function has not been determined (Miyashita-Lin et al., 1999; Hevner et al., 2002). We show here that a significant proportion of thalamic efferents are misrouted caudally and dorsally in $Gbx2^{creER/–}$ embryos (Fig. 1; supplementary material Fig. S1). Furthermore, conditionally deleting *Gbx2* between E9.5 and E14.5 caused similar aberrant trajectories of thalamic efferents (Fig. 2B; Fig. 3B,D; data not

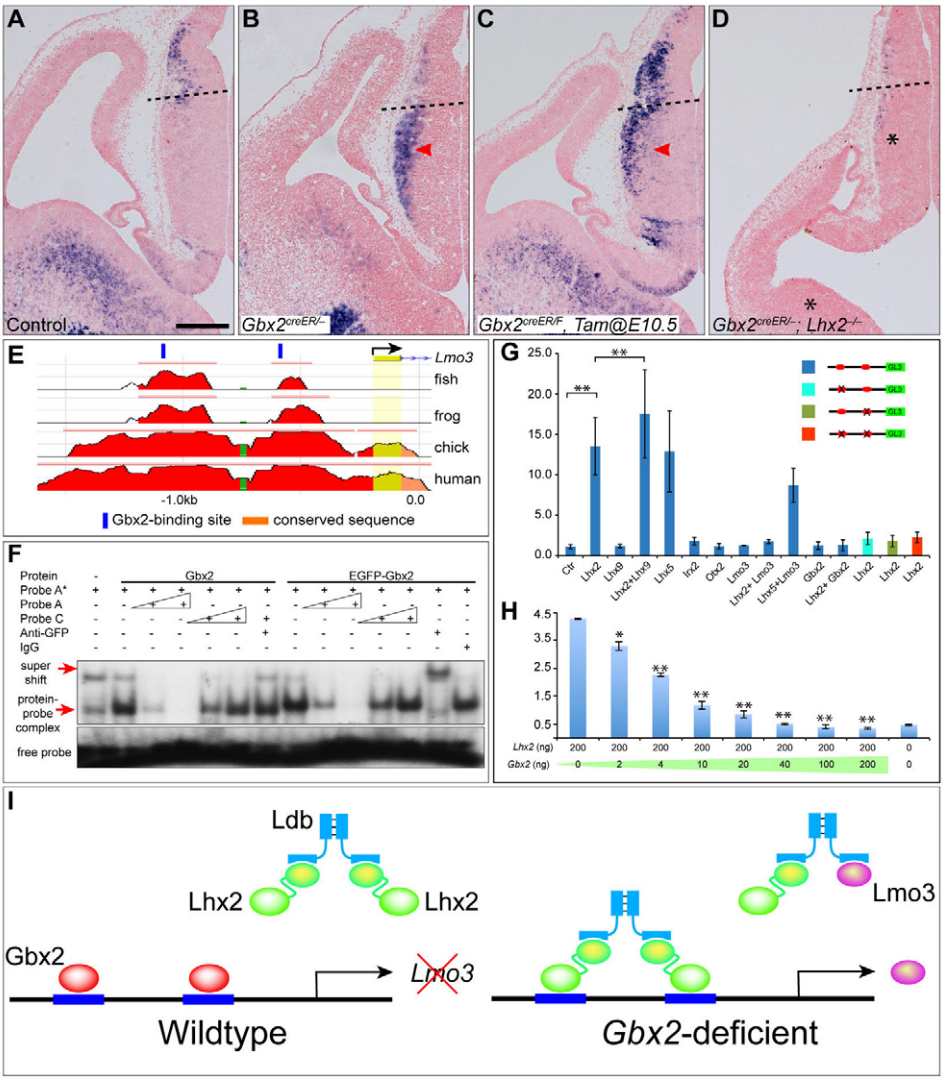

Fig. 5. *Lmo3* is a transcriptional target of Gbx2 and Lhx2. (**A-D**) In situ hybridization of *Lmo3* on coronal sections of E12.5 embryos of indicated genotypes. $Gbx2^{creER/F}$ embryos were given tamoxifen at E10.5. Arrowheads indicate ectopic expression of *Lmo3* in the thalamus; asterisks show lack of *Lmo3* in the thalamus and ventral telencephalon in $Gbx2^{creER/creER}$; $Lhx2^{-/-}$ embryos; broken lines demarcate the dorsal-caudal border of the thalamus. (**E**) Identification of putative Gbx2-binding sites in highly conserved genomic sequence of the mouse *Lmo3* promoter region with VISTA genome browser. (**F**) EMSA analysis of in vitro binding of Gbx2 to the *Lmo3* promoter. Arrows indicate bands corresponding to the protein-DNA complex and super-shifted complex. (**G**,**H**) Luciferase reporter analyses of the activation of the *Lmo3* promoter by Lhx2 and other transcription factors (G), and the inhibition of Lhx2 by Gbx2 (H). The key shows Lmo3-luciferae (GL3) constructs without or with point mutations at the putative Gbx2/Lhx2-binding sites. Co-transfection of *Gbx2,* as little of 1/100 the amount of *Lhx2,* can significantly inhibit Lhx2 activity, and mutating either or both binding sites abolishes the activation of the *Lmo3* promoter by Lhx2. Data are mean±s.d. Asterisks indicate significant differences (**P<0.001, *P<0.05; Student's t-test). (**I**) The regulation of the LIM code by *Gbx2* in thalamic neurons. Gbx2 normally occupies the *Lmo3* promoter, preventing Lhx2 from activating *Lmo3* transcription; in the absence of Gbx2, Lhx2 binds to *Lmo3* promoter and leads to production of Lmo3 proteins, which in turn inhibit Lhx2 function by disrupting the Lhx2-Ldb transcription complex. Scale bar: 250 μm in A-D.

shown). Therefore, *Gbx2* plays a crucial role in establishing the initial axonal trajectory of the newly generated thalamic neurons at different embryonic stages.

Genetic studies have identified numerous molecules that are essential for TCA development (López-Bendito and Molnar, 2003; Seibt et al., 2003; Powell et al., 2008; Dwyer et al., 2011). However, mutant mice lacking any of these molecules apparently do not display the trajectory defect found in *Gbx2* mutants, indicating that *Gbx2* controls an unknown pathway in regulating the initial trajectory of TCAs. In the absence of *Gbx2*, many thalamic efferents are fasciculated with the FR tract and project to the ventral midbrain (Fig. 1B,D; Fig. 3B). The projection pattern of *Gbx2*-deficient thalamic neurons is remarkably similar to that of habenular neurons (Quina et al., 2009). The habenula and thalamus are both derived from the alar plate of a single diencephalic segment, called prosomere 2 (Rubenstein et al., 1994). We have previously shown that *Gbx2* is exclusively expressed in the thalamus, primarily in both neural precursors that are about to exit cell cycle and postmitotic neurons (Chen et al., 2009). Therefore, *Gbx2* may be important for assigning distinct characteristics, such as TCA connectivity, to postmitotic neurons arising from the alar plate of prosomere 2.

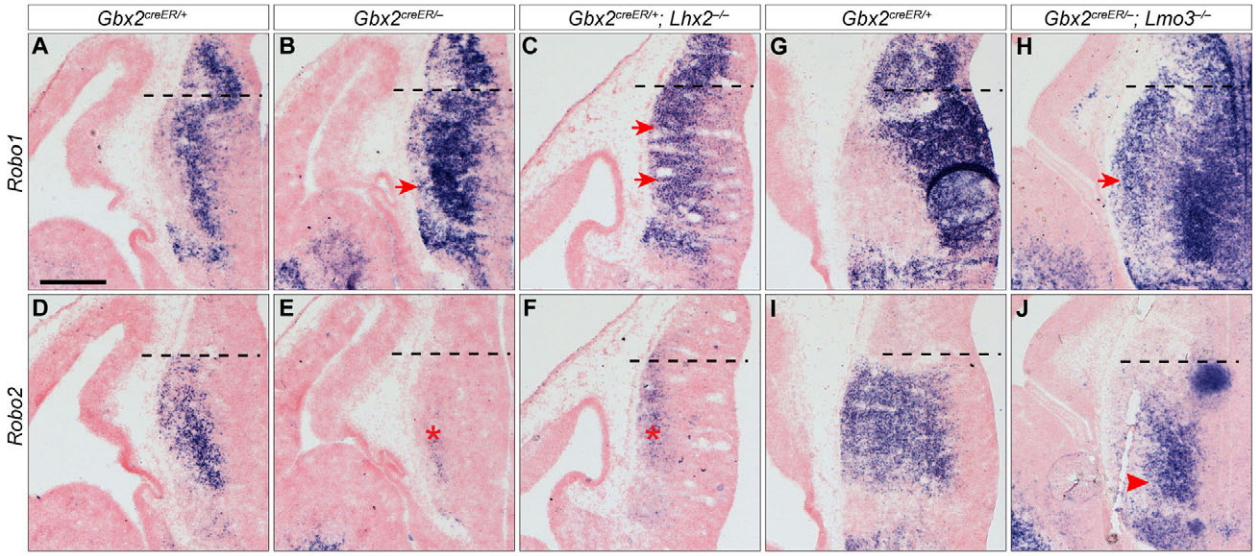

Fig. 6. Gbx2 positively regulates Lhx2 activity in the control of Robo1 and Robo2 expression. In situ hybridization on coronal sections of E12.5 (**A-F**) and E13.5 (**G-J**) embryos. RNA probes and genotypes are indicated to the left and on the top. Broken lines demarcate the dorsal-caudal border of the thalamus; arrows indicate the ectopic expression of *Robo1* in the MZ of the thalamus; asterisks show the reduction of *Robo2*; the arrowhead indicates the rescued Robo2. Scale bar: 250 μm in A-J.

Pathfinding defects of TCAs and abnormal Robo expression in the absence of Gbx2

By using chimera and mosaic analyses, we demonstrate that Gbx2 acts cell-autonomously to control the extension of TCAs into the prethalamus. Furthermore, deleting *Gbx2* after the TCAs have passed the prethalamus led to TCA guidance defects and accelerated invasion into the cortical plate (Fig. 2J). As conditional deletion using creER creates genetic mosaicism (supplementary material Fig. S2) (Chen et al., 2009; Sunmonu et al., 2011), the guidance defects in *Gbx2*-CKO mutants thus reflect a cell-autonomous function of Gbx2. These in vivo studies, together with the explant assays (Fig. 3K-M), clearly demonstrate that *Gbx2* regulates the outgrowth and pathfinding of TCAs by modifying their responsiveness to guidance cues en route to the neocortex.

To control TCA guidance, *Gbx2* probably regulates guidance receptors and intracellular signaling in thalamic neurons and TCAs. In the current study, we have mainly focused on Robo1 and Robo2 because of their important roles in TCA development. The guidance defects of TCAs outside the diencephalon in *Gbx2*-CKO mutants share similarities with those reported in mouse embryos lacking Slit1 and Slit2 or Robo1 and Robo2 (Bagri et al., 2002; Andrews et al., 2006; López-Bendito et al., 2007), as well as in *Lhx2*-CKO mutants that exhibit ectopic expression of *Robo1* (Marcos-Mondejar et al., 2012). Therefore, altered expression of Robo1 and Robo2 probably accounts for the guidance defects found in the telencephalon in *Gbx2*-CKO mutants. Furthermore, studying the regulation of *Robo1/2* has allowed us to define an intricate genetic network regulated by Gbx2 in the developing thalamus. Significantly, it has recently been shown that Slit/Robo interactions play an important role in the topographic sorting of TCAs in the ventral telencephalon (Bielle et al., 2011a). It has been demonstrated that differential expression of *Robo1* and *Robo2* (*robo* and *lea* – FlyBase), which interact with Slit signaling from the midline, determines the lateral position of post-crossing commissural and longitudinal axons in *Drosophila* (Rajagopalan et al., 2000; Simpson et al., 2000). Similarly, the differential expression of Robo1 and Robo2 in different thalamic nuclei may form a Robo code to interpret Slit signals in establishing the TCA topography in the ventral telencephalon. We have previously demonstrated that different thalamic nuclei display distinct and dynamic expression of *Gbx2* (Chen et al., 2009). Therefore, regulating Robo1 and Robo2 receptor levels through Gbx2 activity in TCAs derived from different thalamic nuclei may provide an important mechanism with which to establish the topographic projections of TCAs.

Regulation of the LIM code by Gbx2 leads to differential expression of Robo1 and Robo2 in thalamic neurons

In *Drosophila* wing disc, the Lhx2 homolog *Apterous* induces expression of LMO protein, which in turn represses the activity of Apterous (Milán et al., 1998). In the current study, we have identified a similar feedback mechanism between Lhx2 and Lmo3 in the developing thalamus. Furthermore, we demonstrate that Gbx2 blocks *Lmo3* transcription by competing for the binding of Lhx2 to the *Lmo3* promoter. Therefore, *Gbx2* exerts its regulatory role in the developing thalamus in part by regulating an evolutionarily conserved Apterous-Lmo feedback loop. We show that the positive regulation of Lhx2 activity by Gbx2 is essential for Robo2 expression in the thalamus (Fig. 7K). In contrast to *Lhx2*, *Lhx9* is negatively regulated by Gbx2 at the transcriptional level. Although definitive evidence awaits further study, our data suggest that Lhx9 may mediate Gbx2 function in regulating the expression of *Robo1* (Fig. 7K). We found that the expression patterns of *Lhx9* and *Robo1* in the thalamus almost completely mirrored each other, not only in wild type but also in *Gbx2* mutant embryos (Fig. 7E-J′). Furthermore, removing *Lmo3* had no effects on the ectopic expression of either *Lhx9* or *Robo1* in the *Gbx2*-deficient thalamus (Fig. 7E″-J″). Altogether, these observations suggest that Lhx9 positively regulates *Robo1* expression, and that the mis-regulation of *Lhx9*

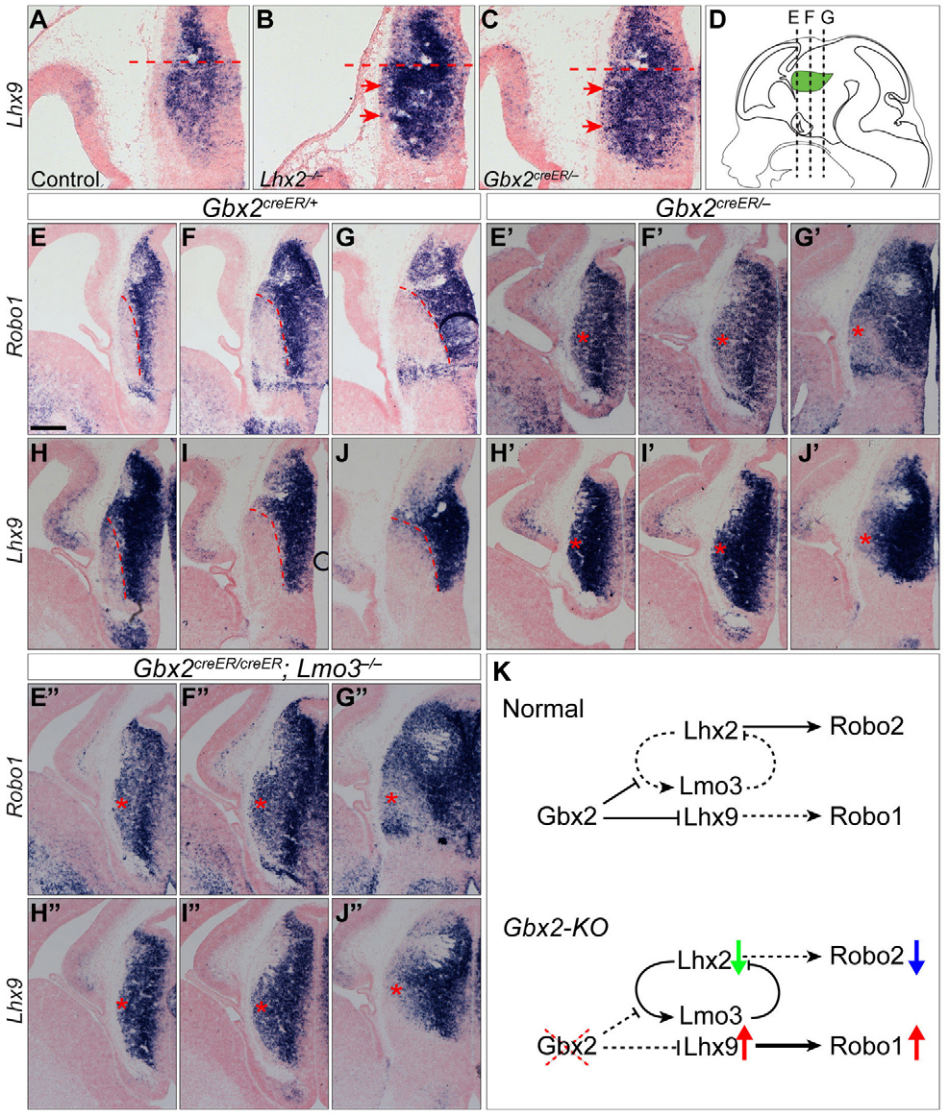

Fig. 7. Gbx2 negatively regulates *Lhx9* transcription in repressing *Robo1* expression. (**A-C**) In situ hybridization for *Lhx9* on coronal sections of E12.5 embryos of indicated genotypes. Broken lines demarcate the dorsal-caudal border of the thalamus; arrows indicate the ectopic expression of *Lhx9* transcripts and proteins in the lateral-most area of the thalamus. (**D-J″**) In situ hybridization for *Robo1* and *Lhx9* on adjacent coronal sections at different levels of the thalamus in E13.5 embryos of indicated genotypes. The relative positions of the sections (broken lines) are shown in the schematic drawing in D. Red dashed lines demarcate the negative domain of *Robo1* and *Lhx9* in the thalamus; asterisks indicate the ectopic expression of *Robo1* and *Lhx9*. (**K**) Summary of the regulation of Robo1 and Robo2 in the thalamus with or without Gbx2. Broken lines indicate the loss or reduced activity. Arrows in green, blue and red indicate reduced activity, reduced transcription and enhanced transcription, respectively. Scale bar: 147 μm in A-C; 250 μm in E-J″.

in *Gbx2*-deficient thalamus may be responsible for the ectopic expression of *Robo1* in the same region.

It has been reported that Lhx2 negatively regulates Robo1 and Robo2, probably by direct transcriptional regulation (Marcos-Mondejar et al., 2012). As Lhx2 negatively regulates the expression of *Lhx9* (Fig. 7B), the mis-regulation of *Lhx9* may contribute to the altered expression of *Robo1* following the manipulations of *Lhx2* in the previous study. In contrast to our current findings, it was shown that gain or loss of function of Lhx2 resulted in the reduction or increase, respectively, in the level of *Robo2* expression. Differences in experimental approaches may contribute to this apparent discrepancy. For example, the previous study examined *Robo2* expression only at E14.5, while we have focused on the initial expression of *Robo2*. Importantly, in the previous study, deletion of *Lhx2* was achieved by tamoxifen-induced deletion using the *Gbx2*^{creER} knock-in mouse line after E10.5, whereas gain of function was performed by in utero electroporation at E13.5. As the expression of *Lhx2* and *Gbx2* are initiated in the thalamus around the same time at E10.5, those manipulations will only change *Lhx2* expression after its initially normal expression. Furthermore, those manipulations will alter *Lhx2* expression in thalamic neurons in a mosaic manner. In the current study, we examined *Robo2* transcripts in the thalamus in global *Lhx2*-KO mutants.

In summary, our results demonstrate that *Gbx2* regulates the expression of *Robo2* in the thalamus by repressing *Lmo3* and consequently promoting Lhx2 protein function. Meanwhile, *Gbx2* is essential to repress *Robo1* in the lateral-most area of the thalamus, probably by inhibiting *Lhx9* transcription in this region.

Concluding remarks

Here, we have identified at least three different mechanisms through which Gbx2 modifies the LIM transcriptional code: (1) Gbx2 regulates Lhx2 function by repressing its inhibitor *Lmo3*; (2) Gbx2 competes for binding of Lhx2 to the same DNA sequences of the *Lmo3* promoter; (3) Gbx2 negatively regulates the transcription of *Lhx9*. Although *Gbx2* and *Lhx2* antagonize each other when regulating *Lmo3* expression, they both promote *Robo2* expression. Therefore, the interaction between Gbx2 and Lhx2 must be highly context dependent. It is conceivable that there are many other *Lmo3*-like or *Robo2*-like transcriptional targets that are regulated by both Gbx2 and Lhx2 in the developing thalamus. The relative stoichiometries of Gbx2 and Lhx2 are thus important in conferring distinct identity and connectivity of thalamic neurons.

During embryogenesis, the thalamus is gradually parcellated into multiple nuclei. Each nucleus has distinct cytoarchitecture and function, and projects to a specific set of cortical areas. *Gbx2*, *Lhx2* and *Lhx9* are expressed in discrete and overlapping domains of the thalamus, and different thalamic nuclei display distinctive expression patterns of *Gbx2* (Nakagawa and O'Leary, 2001; Chen et al., 2009). Gbx2 and LIM-HD transcription factors may thus constitute the core of the regulatory network that define the diverse identity and connectivity of thalamic nuclei.

Acknowledgements
We thank Dr Wei Lun Leung for critical reading and comments of the manuscript. We thank Drs Shubha Tole and Edwin Monuki for providing *Lhx2* mutant embryos and mice; Dr Atsushi Tamada for providing the antibodies against Robo1 and Robo2; and Dr Lynda Erskine for providing *SLIT2* expressing vector. The monoclonal anti-NEFM antibody (2H3) was developed by T. M. Jessell and J. Dodd, and obtained through the Developmental Studies Hybridoma Bank under the auspices of the NICHD and maintained by The University of Iowa (Iowa City, IA). We thank Dr Mark Kronenberg for providing reagents and advice on EMSA and luciferase reporter assays.

Funding
This work was supported by grants from the National Institutes of Health [R01MH094914 to J.Y.H.L.]. Deposited in PMC for release after 12 months.

Competing interests statement
The authors declare no competing financial interests.

Supplementary material
Supplementary material available online at
http://dev.biologists.org/lookup/suppl/doi:10.1242/dev.086991/-/DC1

References

Andrews, W., Liapi, A., Plachez, C., Camurri, L., Zhang, J., Mori, S., Murakami, F., Parnavelas, J. G., Sundaresan, V. and Richards, L. J. (2006). Robo1 regulates the development of major axon tracts and interneuron migration in the forebrain. *Development* **133**, 2243-2252.
Bach, I. (2000). The LIM domain: regulation by association. *Mech. Dev.* **91**, 5-17.
Bagri, A., Marín, O., Plump, A. S., Mak, J., Pleasure, S. J., Rubenstein, J. L. and Tessier-Lavigne, M. (2002). Slit proteins prevent midline crossing and determine the dorsoventral position of major axonal pathways in the mammalian forebrain. *Neuron* **33**, 233-248.
Berger, M. F., Badis, G., Gehrke, A. R., Talukder, S., Philippakis, A. A., Peña-Castillo, L., Alleyne, T. M., Mnaimneh, S., Botvinnik, O. B., Chan, E. T. et al. (2008). Variation in homeodomain DNA binding revealed by high-resolution analysis of sequence preferences. *Cell* **133**, 1266-1276.
Bielle, F., Marcos-Mondejar, P., Keita, M., Mailhes, C., Verney, C., Nguyen Ba-Charvet, K., Tessier-Lavigne, M., Lopez-Bendito, G. and Garel, S. (2011a). Slit2 activity in the migration of guidepost neurons shapes thalamic projections during development and evolution. *Neuron* **69**, 1085-1098.
Bielle, F., Marcos- Mondéjar, P., Leyva-Diaz, E., Lokmane, L., Mire, E., Mailhes, C., Keita, M., Garcia, N., Tessier-Lavigne, M., Garel, S. et al. (2011b). Emergent growth cone responses to combinations of Slit1 and Netrin 1 in thalamocortical axon topography. *Curr. Biol.* **21**, 1748-1755.
Bonnin, A., Torii, M., Wang, L., Rakic, P. and Levitt, P. (2007). Serotonin modulates the response of embryonic thalamocortical axons to netrin-1. *Nat. Neurosci.* **10**, 588-597.
Braisted, J. E., Ringstedt, T. and O'Leary, D. D. (2009). Slits are chemorepellents endogenous to hypothalamus and steer thalamocortical axons into ventral telencephalon. *Cereb. Cortex* **19**, i144-i151.
Brose, K., Bland, K. S., Wang, K. H., Arnott, D., Henzel, W., Goodman, C. S., Tessier-Lavigne, M. and Kidd, T. (1999). Slit proteins bind Robo receptors and have an evolutionarily conserved role in repulsive axon guidance. *Cell* **96**, 795-806.
Bulfone, A., Puelles, L., Porteus, M. H., Frohman, M. A., Martin, G. R. and Rubenstein, J. L. (1993). Spatially restricted expression of Dlx-1, Dlx-2 (Tes-1), Gbx-2, and Wnt-3 in the embryonic day 12.5 mouse forebrain defines potential transverse and longitudinal segmental boundaries. *J. Neurosci.* **13**, 3155-3172.
Buratowski, S. and Chodosh, L. A. (2001). Mobility shift DNA-binding assay using gel electrophoresis. *Curr. Protoc. Mol. Biol.* **36**, 12.2.1-12.2.11.
Chen, L., Guo, Q. and Li, J. Y. (2009). Transcription factor Gbx2 acts cell-nonautonomously to regulate the formation of lineage-restriction boundaries of the thalamus. *Development* **136**, 1317-1326.
Chen, L., Chatterjee, M. and Li, J. Y. (2010). The mouse homeobox gene Gbx2 is required for the development of cholinergic interneurons in the striatum. *J. Neurosci.* **30**, 14824-14834.
Dwyer, N. D., Manning, D. K., Moran, J. L., Mudbhary, R., Fleming, M. S., Favero, C. B., Vock, V. M., O'Leary, D. D., Walsh, C. A. and Beier, D. R. (2011). A forward genetic screen with a thalamocortical axon reporter mouse yields novel neurodevelopment mutants and a distinct emx2 mutant phenotype. *Neural Dev.* **6**, 3.
Garel, S. and Rubenstein, J. L. (2004). Intermediate targets in formation of topographic projections: inputs from the thalamocortical system. *Trends Neurosci.* **27**, 533-539.
Hevner, R. F., Miyashita-Lin, E. and Rubenstein, J. L. (2002). Cortical and thalamic axon pathfinding defects in Tbr1, Gbx2, and Pax6 mutant mice: evidence that cortical and thalamic axons interact and guide each other. *J. Comp. Neurol.* **447**, 8-17.
Jones, E. G. (2007). *The Thalamus*. New York, NY: Cambridge University Press.
Jones, E. G. and Rubenstein, J. L. (2004). Expression of regulatory genes during differentiation of thalamic nuclei in mouse and monkey. *J. Comp. Neurol.* **477**, 55-80.
Kain, S. R. and Ganguly, S. (2001). Overview of Genetic Reporter Systems. *Curr. Protoc. Mol. Biol.* **68**, 9.6.1-9.6.12.
Lakhina, V., Falnikar, A., Bhatnagar, L. and Tole, S. (2007). Early thalamocortical tract guidance and topographic sorting of thalamic projections requires LIM-homeodomain gene Lhx2. *Dev. Biol.* **306**, 703-713.
Lee, S., Lee, B., Joshi, K., Pfaff, S. L., Lee, J. W. and Lee, S. K. (2008). A regulatory network to segregate the identity of neuronal subtypes. *Dev. Cell* **14**, 877-889.
Li, J. Y., Lao, Z. and Joyner, A. L. (2002). Changing requirements for Gbx2 in development of the cerebellum and maintenance of the mid/hindbrain organizer. *Neuron* **36**, 31-43.
Loots, G. G., Ovcharenko, I., Pachter, L., Dubchak, I. and Rubin, E. M. (2002). rVista for comparative sequence-based discovery of functional transcription factor binding sites. *Genome Res.* **12**, 832-839.
López-Bendito, G. and Molnár, Z. (2003). Thalamocortical development: how are we going to get there? *Nat. Rev. Neurosci.* **4**, 276-289.
López-Bendito, G., Flames, N., Ma, L., Fouquet, C., Di Meglio, T., Chedotal, A., Tessier-Lavigne, M. and Marín, O. (2007). Robo1 and Robo2 cooperate to control the guidance of major axonal tracts in the mammalian forebrain. *J. Neurosci.* **27**, 3395-3407.
Lund, R. D. and Mustari, M. J. (1977). Development of the geniculocortical pathway in rats. *J. Comp. Neurol.* **173**, 289-305.
Madisen, L., Zwingman, T. A., Sunkin, S. M., Oh, S. W., Zariwala, H. A., Gu, H., Ng, L. L., Palmiter, R. D., Hawrylycz, M. J., Jones, A. R. et al. (2010). A robust and high-throughput Cre reporting and characterization system for the whole mouse brain. *Nat. Neurosci.* **13**, 133-140.
Marcos-Mondéjar, P., Peregrin, S., Li, J. Y., Carlsson, L., Tole, S. and López-Bendito, G. (2012). The lhx2 transcription factor controls thalamocortical axonal guidance by specific regulation of robo1 and robo2 receptors. *J. Neurosci.* **32**, 4372-4385.
Métin, C. and Godement, P. (1996). The ganglionic eminence may be an intermediate target for corticofugal and thalamocortical axons. *J. Neurosci.* **16**, 3219-3235.
Milán, M., Diaz-Benjumea, F. J. and Cohen, S. M. (1998). Beadex encodes an LMO protein that regulates Apterous LIM-homeodomain activity in Drosophila wing development: a model for LMO oncogene function. *Genes Dev.* **12**, 2912-2920.
Miyashita-Lin, E. M., Hevner, R., Wassarman, K. M., Martinez, S. and Rubenstein, J. L. (1999). Early neocortical regionalization in the absence of thalamic innervation. *Science* **285**, 906-909.
Molnar, Z., Adams, R. and Blakemore, C. (1998). Mechanisms underlying the early establishment of thalamocortical connections in the rat. *J. Neurosci.* **18**, 5723-5745.
Nagy, A., Gertsenstein, M., Vintersten, K. and Behringer, R. (2003). *Manipulating the Mouse Embryo*. Cold Spring Harbor, New York: Cold Spring Harbor Laboratory Press.
Nakagawa, Y. and O'Leary, D. D. (2001). Combinatorial expression patterns of LIM-homeodomain and other regulatory genes parcellate developing thalamus. *J. Neurosci.* **21**, 2711-2725.
O'Donnell, M., Chance, R. K. and Bashaw, G. J. (2009). Axon growth and guidance: receptor regulation and signal transduction. *Annu. Rev. Neurosci.* **32**, 383-412.
O'Leary, D. D. and Koester, S. E. (1993). Development of projection neuron types, axon pathways, and patterned connections of the mammalian cortex. *Neuron* **10**, 991-1006.
Porter, F. D., Drago, J., Xu, Y., Cheema, S. S., Wassif, C., Huang, S. P., Lee, E., Grinberg, A., Massalas, J. S., Bodine, D. et al. (1997). Lhx2, a LIM homeobox gene, is required for eye, forebrain, and definitive erythrocyte development. *Development* **124**, 2935-2944.
Powell, A. W., Sassa, T., Wu, Y., Tessier-Lavigne, M. and Polleux, F. (2008). Topography of thalamic projections requires attractive and repulsive functions of Netrin-1 in the ventral telencephalon. *PLoS Biol.* **6**, e116.

Quina, L. A., Wang, S., Ng, L. and Turner, E. E. (2009). Brn3a and Nurr1 mediate a gene regulatory pathway for habenula development. *J. Neurosci.* **29**, 14309-14322.
Rajagopalan, S., Vivancos, V., Nicolas, E. and Dickson, B. J. (2000). Selecting a longitudinal pathway: Robo receptors specify the lateral position of axons in the Drosophila CNS. *Cell* **103**, 1033-1045.
Rakic, P. (1977). Prenatal development of the visual system in rhesus monkey. *Philos. Trans. R. Soc. Lond. B Biol. Sci.* **278**, 245-260.
Rubenstein, J. L., Martinez, S., Shimamura, K. and Puelles, L. (1994). The embryonic vertebrate forebrain: the prosomeric model. *Science* **266**, 578-580.
Seibt, J., Schuurmans, C., Gradwhol, G., Dehay, C., Vanderhaeghen, P., Guillemot, F. and Polleux, F. (2003). Neurogenin2 specifies the connectivity of thalamic neurons by controlling axon responsiveness to intermediate target cues. *Neuron* **39**, 439-452.
Simpson, J. H., Kidd, T., Bland, K. S. and Goodman, C. S. (2000). Short-range and long-range guidance by slit and its Robo receptors. Robo and Robo2 play distinct roles in midline guidance. *Neuron* **28**, 753-766.
Sunmonu, N. A., Li, K., Guo, Q. and Li, J. Y. (2011). Gbx2 and Fgf8 are sequentially required for formation of the midbrain-hindbrain compartment boundary. *Development* **138**, 725-734.
Thaler, J. P., Lee, S. K., Jurata, L. W., Gill, G. N. and Pfaff, S. L. (2002). LIM factor Lhx3 contributes to the specification of motor neuron and interneuron identity through cell-type-specific protein-protein interactions. *Cell* **110**, 237-249.
Tse, E., Smith, A. J., Hunt, S., Lavenir, I., Forster, A., Warren, A. J., Grutz, G., Foroni, L., Carlton, M. B., Colledge, W. H. et al. (2004). Null mutation of the Lmo4 gene or a combined null mutation of the Lmo1/Lmo3 genes causes perinatal lethality, and Lmo4 controls neural tube development in mice. *Mol. Cell. Biol.* **24**, 2063-2073.
Wassarman, K. M., Lewandoski, M., Campbell, K., Joyner, A. L., Rubenstein, J. L., Martinez, S. and Martin, G. R. (1997). Specification of the anterior hindbrain and establishment of a normal mid/hindbrain organizer is dependent on Gbx2 gene function. *Development* **124**, 2923-2934.

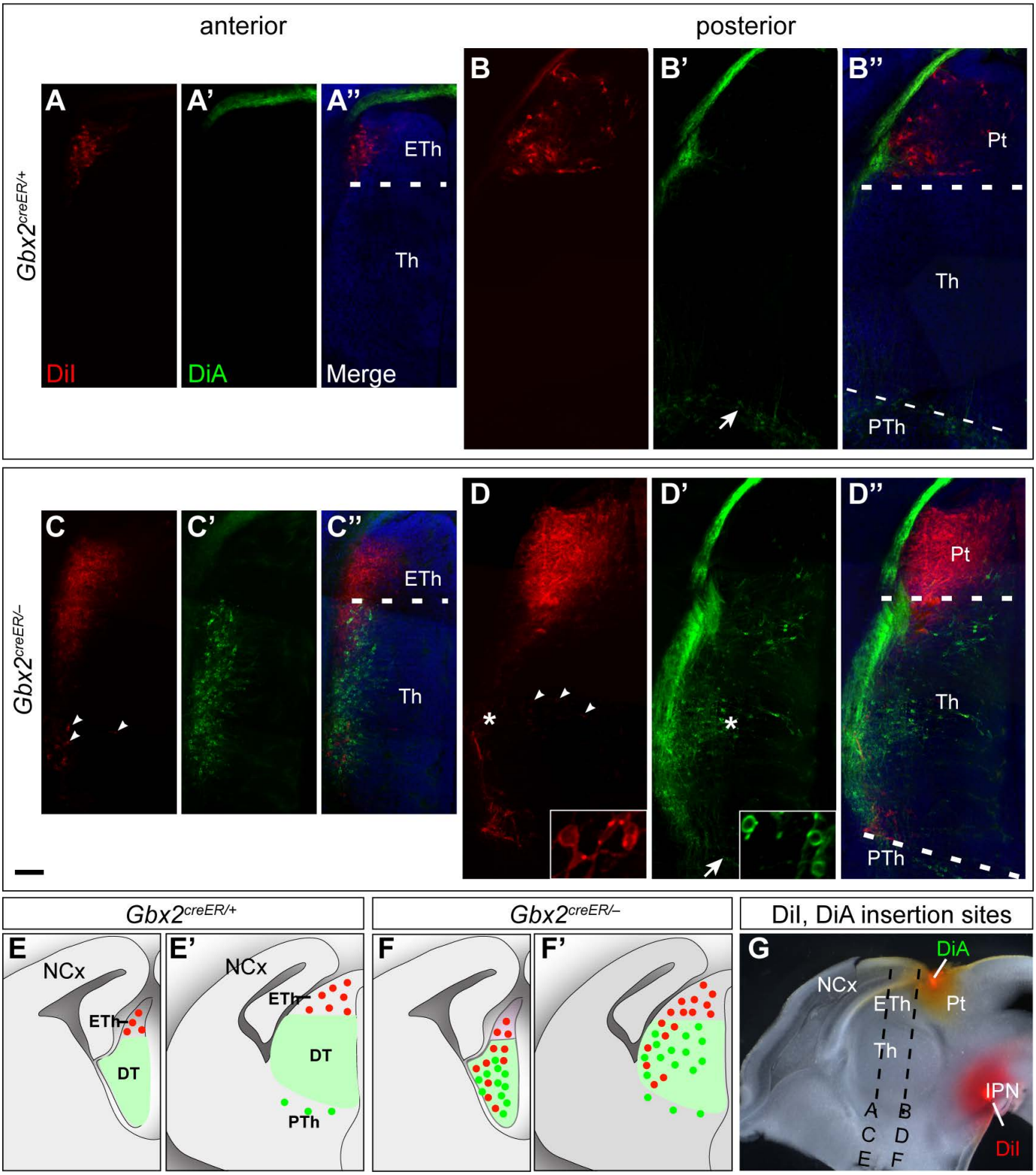

Fig. S1. Analyses of trajectory defects of thalamic axons lacking *Gbx2* using lipophilic dye labeling. (**A-D″**) Confocal images of coronal sections of E14.5 control (A-B″) and *Gbx2*-mutant (C-D″) brains at the anterior and posterior levels. Broken lines indicate the rostral and caudal limits of the thalamus; arrows indicate back-labeled DiA^+ cells in the thalamic reticular nucleus; arrowheads indicate ectopic DiI^+ and DiA^+ neurons, respectively, in the thalamus lacking *Gbx2*; asterisks demarcate cells that are enlarged in insets (D,D′). (**E-F′**) Schematic presentation of the distribution of the back-labeled neurons by DiI (red) and DiA (green). (**G**) Bisected E14.5 brain to show that DiI and DiA crystals are placed in the ventral mesencephalon and dorsal midline of the diencephalon, respectively. Broken lines indicate the plane of sections. Scale bar: 200 μm.

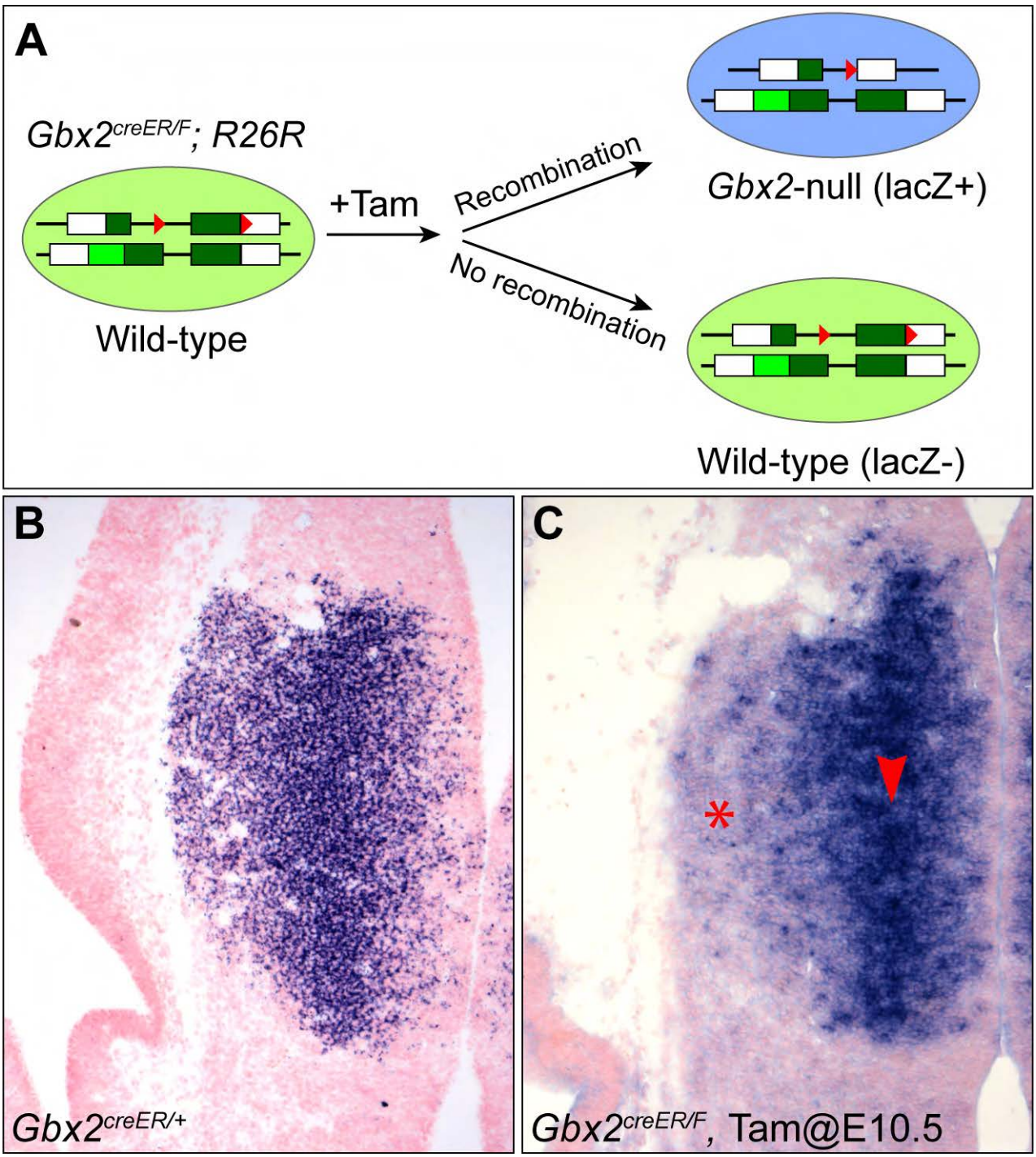

Fig. S2. Generation of *Gbx2* mosaic mutation. (**A**) Schematic representation of the generation of *Gbx2* mosaic mutant thalamus. (**B**,**C**) In situ hybridization using a *Gbx2* RNA probe that recognizes sequence that is deleted by Cre-mediated recombination on coronal section of E12.5 $Gbx2^{creER/+}$ (B) and $Gbx2^{creER/F}$ (C) embryos that received tamoxifen at E10.5. The *Gbx2* expression in the intermediate zone (arrowhead) is unaffected, but is mostly abolished in the mantle zone (asterisk) in $Gbx2^{creER/F}$ embryos.